

See discussions, stats, and author profiles for this publication at: <https://www.researchgate.net/publication/238654174>

# Probing the Electronic Structure and Aromaticity of Pentapnictogen Cluster Anions $Pn_5^-$ ( $Pn = P, As, Sb, \text{ and } Bi$ ) Using Photoelectron Spectroscopy and ab Initio Calculations

ARTICLE in THE JOURNAL OF PHYSICAL CHEMISTRY A · JUNE 2002

Impact Factor: 2.69 · DOI: 10.1021/jp020115k

CITATIONS

70

READS

17

## 4 AUTHORS, INCLUDING:



Lai-Sheng Wang

Brown University

407 PUBLICATIONS 17,419 CITATIONS

SEE PROFILE



Aleksey E. Kuznetsov

Universidade Federal de São Carlos

67 PUBLICATIONS 2,073 CITATIONS

SEE PROFILE



Alexander I Boldyrev

Utah State University

341 PUBLICATIONS 9,841 CITATIONS

SEE PROFILE

# Probing the Electronic Structure and Aromaticity of Pentapnictogen Cluster Anions $\text{Pn}_5^-$ ( $\text{Pn} = \text{P}, \text{As}, \text{Sb}, \text{and Bi}$ ) Using Photoelectron Spectroscopy and *ab Initio* Calculations

Hua-Jin Zhai and Lai-Sheng Wang\*

Department of Physics, Washington State University, 2710 University Drive, Richland, Washington 99352, and W. R. Wiley Environmental Molecular Sciences Laboratory, Pacific Northwest National Laboratory, MS K8-88, P.O. Box 999, Richland, Washington 99352

Aleksey E. Kuznetsov and Alexander I. Boldyrev\*

Department of Chemistry and Biochemistry, Utah State University, Logan, Utah 84322

Received: January 16, 2002; In Final Form: March 26, 2002

The electronic structure and chemical bonding of the pentapnictogen cluster anions,  $\text{Pn}_5^-$  ( $\text{Pn} = \text{P}, \text{As}, \text{Sb}, \text{and Bi}$ ), were investigated using both photoelectron spectroscopy and *ab initio* calculations. Well-resolved photoelectron spectra were obtained for the anions at several photon energies and were analyzed according to the theoretical calculations. The ground state of all the  $\text{Pn}_5^-$  species was found to be the aromatic cyclic  $D_{5h}$  structure with a  $C_{2v}$  low-lying isomer. We found that the  $C_{2v}$  isomer gains stability from  $\text{P}_5^-$  to  $\text{Sb}_5^-$ , consistent with the experimental observation of the coexistence of both isomers in the spectra of  $\text{Sb}_5^-$ . The valence molecular orbitals (MOs) of the  $D_{5h}$   $\text{Pn}_5^-$  were analyzed and compared to those of the aromatic  $\text{C}_5\text{H}_5^-$  hydrocarbon. The same set of  $\pi$ -MOs is shown to be occupied in the  $D_{5h}$   $\text{Pn}_5^-$  and  $\text{C}_5\text{H}_5^-$  species, except that the MO ordering is slightly different. Whereas the three  $\pi$ -MOs in  $\text{C}_5\text{H}_5^-$  all lie above the  $\sigma$ -MOs, the third  $\pi$  orbital ( $1a_2''$  in  $\text{Pn}_5^-$ ) lies below the  $\sigma$ -MOs. The stabilization of the  $\pi$ -MO relative to the  $\sigma$ -MOs seems to be common in inorganic aromatic molecules and distinguishes them from the organic analogues.

## 1. Introduction

The structural and electronic properties of clusters of the pnictogens (Pn) have been of continuing interest. Since the pioneering works done by the groups of Dahl,<sup>1</sup> Ginsberg,<sup>2</sup> and Sacconi<sup>3</sup> in the field of coordinatively stabilized Pn ligands ( $\text{Pn} = \text{P}, \text{As}$ ), rapid developments have taken place in phosphorus and arsenic chemistry.<sup>4–7</sup> Among the various Pn ligands, the pentapnictogen anions,  $\text{Pn}_5^-$ , are particularly interesting.<sup>6,7</sup> The planar cyclic  $\text{P}_5^-$  anion, isovalent with the cyclopentadienyl anion  $\text{C}_5\text{H}_5^-$ , has been prepared in the form of  $\text{MP}_5$  salts ( $\text{M} = \text{Li}, \text{Na}$ ) by Baudler et al.<sup>8,9</sup> It has also been coordinatively stabilized in the form of a stable  $\text{CpFe}(\eta^5\text{-P}_5)$  sandwich complex.<sup>10</sup> Very recently, a carbon-free metallocene  $[(\eta^5\text{-P}_5)_2\text{-Ti}]^{2-}$  has been synthesized.<sup>11</sup>

Gas-phase pnictogen clusters have also been the subject of intensive investigation both theoretically<sup>12–43</sup> and experimentally.<sup>16,32,44–60</sup> In particular, photoelectron spectroscopy (PES) has been performed on the pnictogen clusters.<sup>16,32,44,52,57,58,60</sup> When combined with high level theoretical calculations,<sup>12–16,24–26,28,33,37–39,44</sup> PES of anions could provide a wealth of information on the geometries, electronic structure, vibrational frequencies, and electron affinities of the neutral clusters. A number of previous experimental and theoretical works have been devoted to the  $\text{Pn}_5^-$  clusters.<sup>16,24–26,32,52,58</sup> However, the structures and chemical bonding of these important inorganic species are still not completely understood. In the current work, we report a systematic characterization of the series of pentapnictogen cluster anions  $\text{Pn}_5^-$  ( $\text{Pn} = \text{P}, \text{As}, \text{Sb}$ ,

and Bi) by a combined PES and *ab initio* study with a special interest of their aromaticity. The rich and well-resolved PES features and the excellent agreement between the experiment and theory allow the structural and chemical bonding properties of the  $\text{Pn}_5^-$  species to be thoroughly elucidated. The aromaticity in the  $\text{Pn}_5^-$  clusters was compared to that in the isovalent and classical aromatic molecule,  $\text{C}_5\text{H}_5^-$ .

We have been interested in exploring and characterizing gaseous nonstoichiometric molecules,<sup>61</sup> where novel chemical bonding exists in contradiction to classical stoichiometry. As a serendipitous discovery, we observed all-metal aromatic  $\text{Al}_4^{2-}$  in bimetallic clusters  $\text{MAL}_4^-$  ( $\text{M} = \text{Li}, \text{Na}, \text{and Cu}$ ).<sup>62</sup> We also prepared the analogous aromatic  $\text{NaGa}_4^-$  and  $\text{NaIn}_4^-$  species.<sup>63</sup> We further observed aromaticity in heteroclusters  $\text{MAL}_3^-$  ( $\text{M} = \text{Si}, \text{Ge}, \text{Sn}, \text{and Pb}$ )<sup>64</sup> and explored the aromaticity in  $\text{Hg}_4^{6-}$ ,<sup>65</sup> which are all isoelectronic to  $\text{Al}_4^{2-}$ . The present work represents our continuing interest in exploring aromaticity in inorganic systems.

## 2. Experimental Method

The experiments were carried out using a magnetic-bottle time-of-flight (TOF) photoelectron spectrometer coupled with a laser vaporization supersonic cluster source, details of which have been described previously.<sup>66,67</sup> The  $\text{Pn}_5^-$  ( $\text{Pn} = \text{P}, \text{As}, \text{Sb}, \text{and Bi}$ ) clusters were produced by laser vaporization of the corresponding Pn targets in the presence of a pure helium carrier gas. Various clusters were formed in the source and were mass analyzed using a TOF mass spectrometer. The  $\text{Pn}_5^-$  species of interest were mass-selected and decelerated before being photodetached. Three detachment photon energies were used in the current study, 355 nm (3.496 eV), 266 nm (4.661 eV), and 193

\* Corresponding authors. E-mail (Wang): ls.wang@pnl.gov. E-mail (Boldyrev): boldyrev@cc.usu.edu.

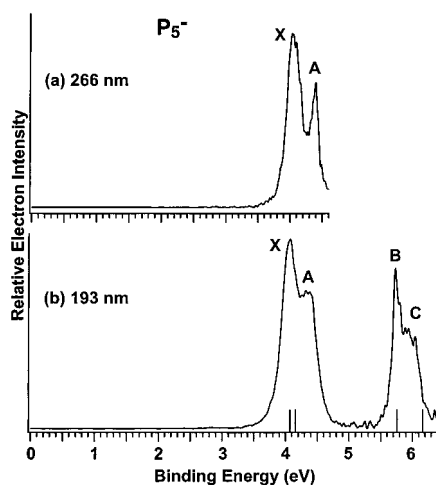


**Figure 1.** Photoelectron spectra of  $\text{P}_5^-$  at (a) 266 nm, and (b) 193 nm. The vertical bars mark the calculated vertical electron detachment energies from the  $D_{5h}$  ground state of  $\text{P}_5^-$ .

nm (6.424 eV). The higher photon energy (6.424 eV) used in the current work allowed much more neutral excited states to be accessed. The higher spectral resolution afforded by the low photon energies (355 and 266 nm) allowed the accessible electronic transitions to be better resolved, yielding more accurate electron affinities and electron binding energies. The photoelectron spectra were calibrated using the known spectrum of  $\text{Rh}^-$ ,<sup>68</sup> and the resolution of the apparatus was better than 30 meV for 1 eV electrons.

### 3. Theoretical Methods

We performed ab initio calculations on a wide variety of structures for  $\text{Pn}_5^-$  to search for the global minimum. We initially optimized geometries and calculated frequencies of  $\text{Pn}_5^-$  ( $\text{Pn} = \text{P}, \text{As}, \text{and Sb}$ ) using analytical gradients with polarized split-valence basis sets (6-311+G\*)<sup>69–71</sup> for P and As and analytical gradients with polarized split-valence basis sets (3-21G\*)<sup>71–77</sup> extended by a set of 2s, 2p, and 1d diffuse functions (3-21G\*+2s2p1d;  $\alpha_{1sp} = 0.0289$ ,  $\alpha_{2sp} = 0.0096$ ;  $\alpha_{1d} = 0.0703$ ) for Sb and a hybrid method known in the literature as B3LYP.<sup>78–80</sup> Two of the most stable structures of  $\text{P}_5^-$  and one of  $\text{As}_5^-$  were further optimized using the coupled-cluster method [CCSD(T)]<sup>81–83</sup> with the 6-311+G\* basis sets. Then the energies of the most stable structures were refined using the CCSD(T) method and the more extended 6-311+G(2df) basis sets. Two of the most stable structures of  $\text{Sb}_5^-$  were calculated using the coupled-cluster method [CCSD(T)] with the 3-21G\*+2s2p1d basis sets. The vertical electron detachment energies (VDEs) were calculated using the outer valence Green Function method<sup>84–88</sup> [OVGF/6-311+G(2df)] and CCSD(T)/6-311+G\* geometries for  $\text{Pn}_5^-$  ( $\text{Pn} = \text{P}$  and As) and [OVGF/3-21G\*+2s2p1d] and B3LYP/3-21G\*+2s2p1d geometries for  $\text{Sb}_5^-$ . Core electrons were kept frozen in treating the electron correlation at the CCSD(T), and the OVGF levels of theory. All calculations were performed using the Gaussian 98 program.<sup>89</sup> Molecular orbitals (MOs) for  $\text{C}_5\text{H}_5^-$  and  $\text{As}_5^-$  were calculated at the RHF/6-311+G\* level of theory. All MO pictures were made using the MOLDEN 3.4 program.<sup>90</sup>

### 4. Experimental Results

Figures 1–4 show the PES spectra of  $\text{Pn}_5^-$  ( $\text{Pn} = \text{P}, \text{As}, \text{Sb}, \text{and Bi}$ ), respectively. Numerous well-resolved PES features were observed for each species, representing transitions from

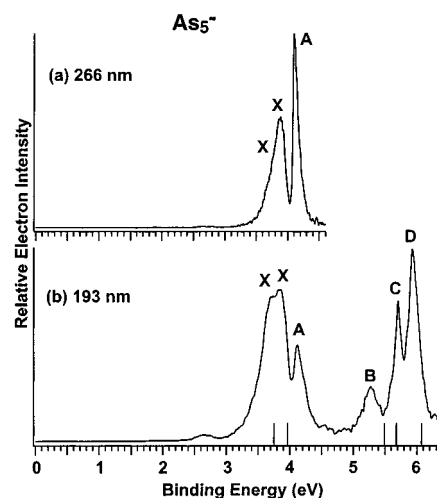


**Figure 2.** Photoelectron spectra of  $\text{As}_5^-$  at (a) 266 nm, and (b) 193 nm. The vertical bars mark the calculated vertical electron detachment energies from the  $D_{5h}$  ground state of  $\text{As}_5^-$ .

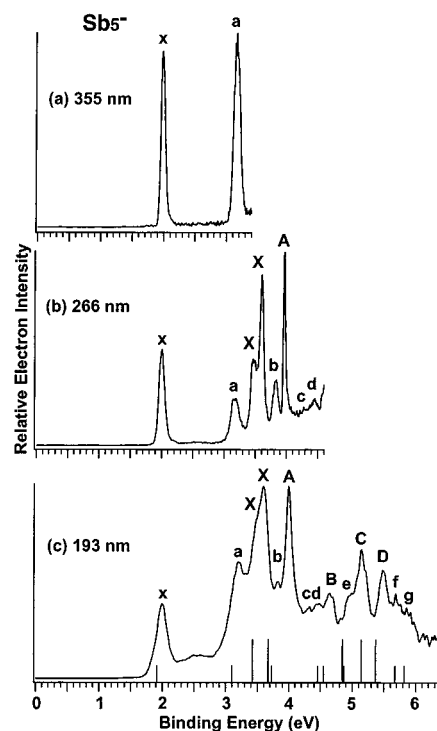


**Figure 3.** Photoelectron spectra of  $\text{Sb}_5^-$  at (a) 355 nm, (b) 266 nm, and (c) 193 nm. The longer vertical bars mark the calculated vertical electron detachment energies from the  $D_{5h}$  ground state of  $\text{Sb}_5^-$ , and the shorter vertical bars mark those from the  $C_{2v}$  low-lying isomer.

the  $\text{Pn}_5^-$  anions to the various states of the  $\text{Pn}_5$  neutrals. The spectra of  $\text{P}_5^-$  (Figure 1) revealed four well-resolved features (X, A, B, and C) with very high electron binding energies. Six well-resolved features were observed for  $\text{As}_5^-$  (X, X', A–D, Figure 2). The weak feature observable in the 193 nm spectrum of  $\text{As}_5^-$  around 2.6 eV (Figure 2b) was shown to be due to a fragmentation process of the parent anion, as discussed later. The spectra of the two heavier  $\text{Pn}_5^-$  species ( $\text{Pn} = \text{Sb}$  and Bi) showed many more features, which were all well resolved and relatively sharp. As will be shown later by comparing the experimental data with theoretical results, two isomers were in fact present for  $\text{Sb}_5^-$ . The VDEs of all the observed spectral features were determined from the peak maxima and are given in Table 1 for all four species. These data are compared with

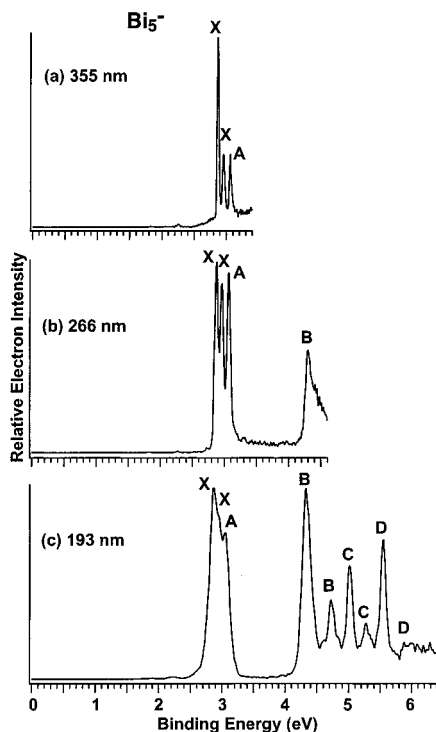


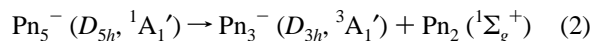
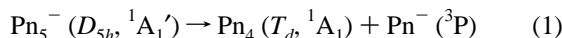
**Figure 4.** Photoelectron spectra of  $\text{Bi}_5^-$  at (a) 355 nm, (b) 266 nm, and (c) 193 nm.

the results of the ab initio calculations (also shown in Table 1), which will be discussed later.

## 5. Theoretical Results

We found that the most stable structure for  $\text{Pn}_5^-$  ( $\text{Pn} = \text{P}, \text{As}, \text{and Sb}$ ) is the cyclic  $D_{5h}$  structure, as shown in Figure 5. All the  $\text{Pn}_5^-$  species were also found to possess a  $C_{2v}$  bridged-roof low-lying singlet isomer. The optimized geometries and relative energies agreed well at the B3LYP and CCSD(T) levels of theory for  $\text{P}_5^-$  and  $\text{As}_5^-$ . Thus, we decided to limit the  $\text{Sb}_5^-$  calculations only to the B3LYP/3-21G\*+2s2p1d level of theory. At our highest level of theory, the global minimum  $D_{5h}$  planar cyclic  $\text{Pn}_5^-$  structure is more stable than the  $C_{2v}$  bridged-roof structure by 33.4, 20.0, and 8.2 kcal/mol for  $\text{Pn} = \text{P}, \text{As}, \text{and Sb}$ , respectively.

We also calculated the energies of the following reactions



for  $\text{Pn} = \text{P}, \text{As}, \text{and Sb}$  at the CCSD(T)/6-311+G(2df) level of theory for P and As and at the CCSD(T)/3-21G\*+2s2p1d level of theory for Sb in order to evaluate the stability of the anions toward dissociation. The calculated energies for the first reaction were found to be: 121.4 kcal/mol for P, 106.6 kcal/mol for As, and 91.0 kcal/mol for Sb; the calculated energies for the second reaction were: 75.8 kcal/mol for P, 68.2 kcal/mol for As, and 70.6 kcal/mol for Sb.

## 6. Interpretation of the Experimental Spectra

Theoretical calculations of the first five detachment processes for the  $D_{5h}$  global minimum structures and the first eight detachment channels for the  $C_{2v}$  isomers were performed for  $\text{Pn}_5^-$  ( $\text{Pn} = \text{P}, \text{As}, \text{Sb}$ ) and are compared with the experimental VDEs in Table 1. The pole strengths, given in the parentheses

**TABLE 1: Experimental and Theoretical Adiabatic (ADE) and Vertical (VDE) Detachment Energies in eV for  $\text{P}_5^-$ ,  $\text{As}_5^-$ ,  $\text{Sb}_5^-$ , and  $\text{Bi}_5^-$**

exptl feature	exptl ADE <sup>a</sup>	exptl VDE <sup>a</sup>	<i>D</i> <sub>5h</sub>		<i>C</i> <sub>2v</sub>	
			MO	theor VDE <sup>b</sup>	MO	theor VDE <sup>b</sup>
<i>P</i> <sub>5</sub> <sup>−</sup>						
X	3.88 (3)	4.05 (3)	1e <sub>1</sub> ''	4.07 (0.87)	3b <sub>1</sub>	1.87 (0.89)
A		4.39 (2)	2e <sub>1</sub> '	4.15 (0.88)	3b <sub>2</sub>	3.23 (0.89)
B		5.72 (4)	2e <sub>2</sub> '	5.76 (0.87)	6a <sub>1</sub>	4.15 (0.88)
C		5.95 (8)	1a <sub>2</sub> ''	6.16 (0.80)	1a <sub>2</sub>	5.33 (0.88)
			2a <sub>1</sub> '	6.87 (0.83)	2b <sub>1</sub>	5.41 (0.86)
					5a <sub>1</sub>	5.74 (0.87)
					4a <sub>1</sub>	6.99 (0.85)
					2b <sub>2</sub>	7.21 (0.87)
<i>As</i> <sub>5</sub> <sup>−</sup>						
X	~ 3.5 (1)	3.75 (5)	1e <sub>1</sub> ''	3.75 (0.87)	3b <sub>1</sub>	1.86 (0.89)
X'		3.88 (2)			3b <sub>2</sub>	3.27 (0.88)
A		4.12 (2)	2e <sub>1</sub> '	3.96 (0.88)	5a <sub>1</sub>	3.95 (0.88)
B		5.28 (4)	1a <sub>2</sub> ''	5.50 (0.79)	1a <sub>2</sub>	4.86 (0.88)
C		5.70 (3)	2e <sub>2</sub> '	5.69 (0.88)	2b <sub>1</sub>	4.98 (0.86)
D		5.92 (3)	2a <sub>1</sub> '	6.07 (0.83)	4a <sub>1</sub>	5.35 (0.87)
					2b <sub>2</sub>	6.50 (0.87)
					3a <sub>1</sub>	6.37 (0.85)
<i>Sb</i> <sub>5</sub> <sup>−</sup>						
X	3.46 (3)	3.46 (3)	1e <sub>1</sub> ''	3.42 (0.87)		
X'		3.60 (3)				
A		3.97 (2)	2e <sub>1</sub> '	3.68 (0.88)		
B		4.65 (5)	1a <sub>2</sub> ''	4.84 (0.78)		
C		5.14 (4)	2e <sub>2</sub> '	5.15 (0.88)		
D		5.48 (4)	2a <sub>1</sub> '	5.37 (0.83)		
x	1.99 (3)	1.99 (3)			3b <sub>1</sub>	1.90 (0.88)
a		3.17 (2)			3b <sub>2</sub>	3.08 (0.89)
b		3.82 (2)			6a <sub>1</sub>	3.72 (0.88)
c		4.32 (5)			1a <sub>2</sub>	4.45 (0.89)
d		4.44 (5)			2b <sub>1</sub>	4.55 (0.86)
e		4.95 (5)			5a <sub>1</sub>	4.86 (0.87)
f		5.70 (5)			4a <sub>1</sub>	5.69(0.86)
g		5.87 (5)			2b <sub>2</sub>	5.81 (0.93)
<i>Bi</i> <sub>5</sub> <sup>−</sup>						
X	2.87 (2)	2.87 (2)				
X'		2.96 (2)				
A		3.06 (2)				
B		4.33 (2)				
B'		4.72 (4)				
C		5.02 (4)				
C'		5.27 (4)				
D		5.55 (4)				
D'		5.95 (5)				

<sup>a</sup> The numbers in the parentheses represent the experimental uncertainty in the last digit. <sup>b</sup> The VDEs were calculated at the OVGF/6-311+G(2df)//CCSD(T)/6-311+G\* level of theory for  $\text{P}_5^-$  and  $\text{As}_5^-$  structures and at the OVGF/3-21G\*+2s2p1d//B3LYP/3-21G\*+2s2p1d level of theory for  $\text{Sb}_5^-$  structures. The numbers in the parentheses indicate the pole strength, which characterizes the validity of the one-electron detachment picture.

in Table 1, are larger than 0.8 for all the calculated detachment channels, implying that the OVGF method is valid and all the electron detachment channels can be considered as primarily one-electron processes. Excellent overall agreement between the experimental photoelectron spectra and the theoretical calculations make the interpretation of the PES data straightforward. The  $D_{5h}$  species were responsible for all the observed PES features for  $\text{P}_5^-$  and  $\text{As}_5^-$ , whereas both the  $D_{5h}$  and  $C_{2v}$  isomers were shown to exist in the spectra of  $\text{Sb}_5^-$ . Jahn–Teller effect and spin–orbit effect are responsible for the fine features observed. More detailed interpretation of the PES data is given below.

**6.1.  $\text{P}_5^-$ .** The four observed PES features (X, A, B, and C) for  $\text{P}_5^-$  were in excellent agreement with the four lowest-lying

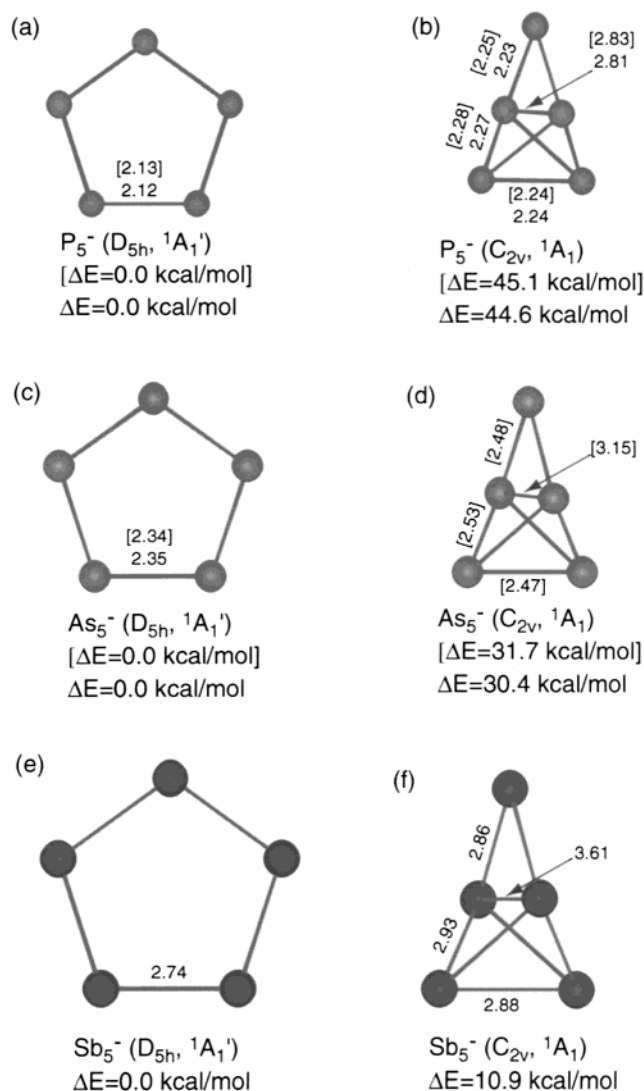


**Figure 5.** Optimized structures of (a)  $\text{P}_5^-$  ( $D_{5h}$ ,  $1A_1'$ ) and (b)  $\text{P}_5^-$  ( $C_{2v}$ ,  $1A_1$ ), (c)  $\text{As}_5^-$  ( $D_{5h}$ ,  $1A_1'$ ) and (d)  $\text{As}_5^-$  ( $C_{2v}$ ,  $1A_1$ ) at the B3LYP/6-311+G\* and CCSD(T)/6-311+G\* levels of theory, and (e)  $\text{Sb}_5^-$  ( $D_{5h}$ ,  $1A_1'$ ) and (f)  $\text{Sb}_5^-$  ( $C_{2v}$ ,  $1A_1$ ) at the B3LYP/3-21G\*+2s2p1d level of theory. Data at the B3LYP/6-311+G\* level of theory are given in brackets. Bond lengths are given in Å.

one-electron detachment channels calculated for the  $D_{5h}$  structure (Figure 1b and Table 1). The fifth theoretical one-electron detachment channel (6.87 eV) is beyond our highest photon energy range (6.424 eV). Since no vibrational structures were resolved for the  $X$  band, the adiabatic detachment energy (ADE) of  $\text{P}_5^-$  was evaluated by drawing a straight line at the leading edge of the  $X$  band and adding a constant to the intersection with the binding energy axis to take into account the instrumental resolution and a finite thermal effect. This procedure yielded the ADE of 3.88 eV for  $\text{P}_5^-$ . The electron binding energies of  $\text{P}_5^-$  is much higher than its neighbors  $\text{P}_4^-$  and  $\text{P}_6^-$  (not shown),<sup>16</sup> whose ground-state PES features have VDEs of  $\sim 1.4$  and  $\sim 2.2$  eV, respectively, indicating that  $\text{P}_5^-$  is an unusually stable cluster species, consistent with its aromatic nature. The width of feature  $X$  is much broader than the instrumental resolution, indicating a structural change from the anion to the neutral state. This is indeed the case: while the anion ground state is  $D_{5h}$ , the neutral state is of  $C_{2v}$  symmetry, mainly due to the Jahn–Teller effect.<sup>13</sup>

The  $C_{2v}$  isomer gave much lower binding energies, according to the theoretical calculations (Table 1). This isomer was not

present in our cluster beam, in agreement with the high relative energy (33.4 kcal/mol) of the  $C_{2v}$  isomer.

**6.2.  $\text{As}_5^-$ .** The observed PES features for  $\text{As}_5^-$  are in good agreement with the first five one-electron detachment channels calculated for the  $D_{5h}$  ground-state structure, as shown in Figure 2b (vertical bars) and Table 1. The first two adjacent features ( $X$  and  $X'$ ) were probably due to the Jahn–Teller splitting because of the doubly degenerate nature of the HOMO ( $1e''$ ) of  $\text{As}_5^-$ . The ground-state feature  $X$  defined an ADE of  $\sim 3.5$  eV for  $\text{As}_5^-$  and a VDE of 3.75 eV. We found that  $\text{As}_5^-$  has a significantly enhanced stability relative to its neighbors  $\text{As}_4^-$  (with a ground-state VDE of  $\sim 1.45$  eV, PES data not shown) and  $\text{As}_6^-$  (with a ground-state VDE of  $\sim 2.05$  eV, PES data not shown), similar to  $\text{P}_5^-$ . The excellent agreement between the experimental and theoretical VDEs confirmed unequivocally the  $D_{5h}$  ground-state structure of  $\text{As}_5^-$  and its aromatic character.

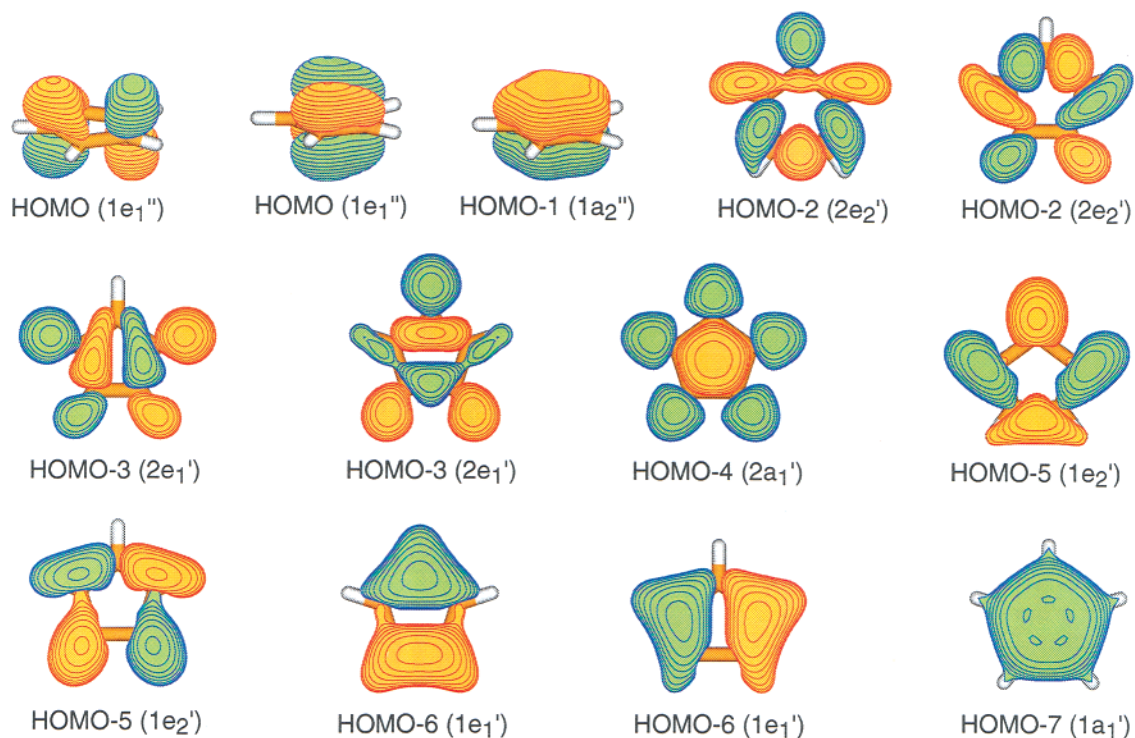
Similar to the case of  $\text{P}_5^-$ , the calculated VDEs for the  $C_{2v}$  isomer of  $\text{As}_5^-$  did not fit our PES data, suggesting that this isomer was not populated in our beam. This is consistent with the high energy of this isomer (20.0 kcal/mol) relative to the  $D_{5h}$  ground state. The weak feature around 2.6 eV observable in the 193 nm (Figure 2b) was not due to the  $C_{2v}$  isomer. This feature was likely due to photofragmentation of the parent  $\text{As}_5^-$ , consistent with the calculated dissociation energy (2.95 eV). Similar spectral features were observed previously in PES spectra of  $\text{P}_5^-$ .<sup>16</sup>

**6.3.  $\text{Sb}_5^-$ .** The PES spectra of  $\text{Sb}_5^-$  (Figure 3), measured at three wavelengths (355, 266, and 193 nm), appeared much more complicated, compared with those of  $\text{P}_5^-$  and  $\text{As}_5^-$ . As shown in Figure 3, fourteen PES features could be identified, with all the VDEs given in Table 1. The complexity and dissimilarity between the  $\text{Sb}_5^-$  spectra to those of the lighter  $\text{Pn}_5^-$  clusters suggested the existence of isomers. Our theoretical calculations showed that the ground state of  $\text{Sb}_5^-$  is the  $D_{5h}$  structure, similar to those of  $\text{P}_5^-$  and  $\text{As}_5^-$ . However, the  $C_{2v}$  isomer of  $\text{Sb}_5^-$  (Figure 5f) is only 8.2 kcal/mol higher in energy, much closer to the ground state. Indeed, the calculated VDEs for the  $D_{5h}$   $\text{Sb}_5^-$  and  $C_{2v}$   $\text{Sb}_5^-$  can account for all the PES features and the theoretical VDEs are in excellent agreement with experimental data, as shown in Figure 3c and Table 1. The six “main” features, labeled as  $X$ ,  $X'$ ,  $A$ ,  $B$ ,  $C$ , and  $D$ , were pretty similar to those of  $\text{As}_5^-$ , and agree well with the five theoretical one-electron detachment channels from the  $D_{5h}$  species. The well-resolved and well-separated features  $X$  and  $X'$  were again attributed to the Jahn–Teller splitting, similar to those in the spectra of  $\text{As}_5^-$ , as discussed above. Feature  $X$  defined a VDE of 3.46 eV for the ground state of the  $D_{5h}$   $\text{Sb}_5^-$  anion, and an ADE of 3.46 eV for  $\text{Sb}_5^-$ . The eight “minor” features ( $x$ ,  $a$ ,  $b$ ,  $c$ ,  $d$ ,  $e$ ,  $f$ , and  $g$ ) in Figure 3 were attributed to the eight theoretical one-electron detachment channels from the  $C_{2v}$  species. The overall agreement between the theory and experiment for both the  $D_{5h}$  and  $C_{2v}$  isomers was excellent, giving considerable credence to the spectral assignments and the theoretical results.

**6.4.  $\text{Bi}_5^-$ .** The PES spectra of  $\text{Bi}_5^-$  at 355, 266, and 193 nm were shown in Figure 4. A total of nine well-resolved and quite sharp features were observed, with their VDEs given in Table 1. We did not carry out ab initio calculations on  $\text{Bi}_5^-$ , because we could not include the relativistic effect in our current level of theory. However, we suspect that the ground-state structure of  $\text{Bi}_5^-$  is likely to be  $D_{5h}$ , similar to the lighter  $\text{Pn}_5^-$  clusters. The spectral patterns of  $\text{Bi}_5^-$  bear some similarities to those of  $\text{P}_5^-$  and  $\text{As}_5^-$ , consistent with the suggestion that they all should



### Molecular Orbitals of the $\text{C}_5\text{H}_5^-$ Species ( $D_{5h}$ , $^1A_1'$ )



### Molecular Orbitals of the $\text{As}_5^-$ Species ( $D_{5h}$ , $^1A_1'$ )

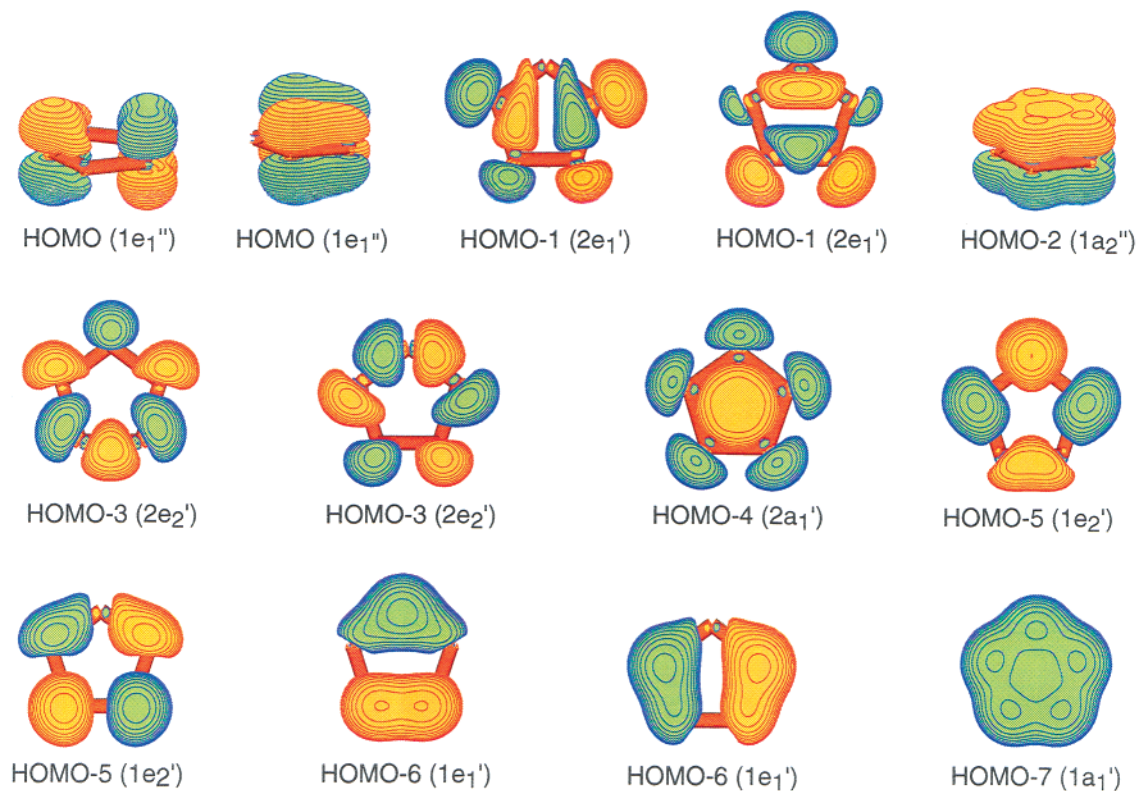


**Figure 6.** Molecular orbital pictures of  $\text{C}_5\text{H}_5^-$  ( $D_{5h}$ ,  $^1A_1'$ ) and  $\text{As}_5^-$  ( $D_{5h}$ ,  $^1A_1'$ ) species.

have similar structures. Relativistic effects are important in Bi atom and clusters, as well documented by the theoretical works of Balasubramanian and co-workers.<sup>37–39</sup> The rich spectral

features presented here for  $\text{Bi}_5^-$  suggest that it would be interesting to perform further theoretical calculations on this system with the relativistic effects explicitly included.

## 7. Characterization of the Aromaticity in the $D_{5h}$ $\text{Pn}_5^-$ Clusters

The excellent agreement between the observed PES features and the ab initio calculations presented herein firmly established that the  $D_{5h}$  cyclic structure is the global minimum for all the  $\text{Pn}_5^-$  anions investigated here. These cluster anions were found to be unusually stable electronically, as indicated by their high electron binding energies. This unusual electronic stability derives from both the closed shell nature of the  $\text{Pn}_5^-$  clusters and their aromaticity, which will be discussed next.

The  $D_{5h}$   $\text{Pn}_5^-$  anions are isovalent to the classical aromatic cyclopentadienyl  $\text{C}_5\text{H}_5^-$  anion. Figure 6 displays the thirteen valence molecular orbitals of the  $D_{5h}$   $\text{As}_5^-$ , compared to those of the  $D_{5h}$   $\text{C}_5\text{H}_5^-$ . The similarity between the MOs of the two anions is obvious. The MO pictures show clearly six delocalized  $\pi$  electrons for  $\text{As}_5^-$  in the  $1e_1''$  and  $1a_2''$  orbitals, which fulfill the  $(4n + 2)$  Hückel rule for classical aromaticity. The order of the MOs for the two species corresponds to the ones given by the OVGf method, at the OVGf/6-311+G(2df) level of theory for  $\text{As}_5^-$  and the OVGf/6-311++G(2df,2pd) level of theory for  $\text{C}_5\text{H}_5^-$  species. The three aromatic  $\pi$ -MOs are identical in both anions, except that their orders differ. In  $\text{C}_5\text{H}_5^-$ , the  $\pi$ -aromatic  $1a_2''$  MO is 0.67 eV higher in energy than the highest degenerate  $\sigma$ -MO ( $2e_2'$ ), while in  $\text{As}_5^-$  the analogous  $1a_2''$  MO is 1.54 eV lower in energy than the highest degenerate  $\sigma$ -MO ( $2e_1'$ ). Thus, in the case of the aromatic hydrocarbon  $\text{C}_5\text{H}_5^-$ , the  $\sigma$ -MOs are filled before the  $\pi$ -MOs. But in the case of  $\text{As}_5^-$ , the  $\pi$ -aromatic  $1a_2''$  MO (HOMO-2) is lower in energy than the  $2e_1'$  (HOMO-1)  $\sigma$ -MOs, and thus the  $\pi$ -MO is filled before the  $\sigma$ -MOs. Similar situations were found in  $\text{P}_5^-$  and  $\text{Sb}_5^-$  (Table 1). In the case of  $\text{P}_5^-$ , the  $\pi$ -aromatic  $1a_2''$  MO is lower in energy even more: it becomes separated from the  $1e_1''$   $\pi$ -MOs by two degenerate  $\sigma$ -MOs. Such behavior makes inorganic aromatic compounds different from the organic analogues. The same tendency to fill  $\pi$ -aromatic MOs before the  $\sigma$ -MOs have also been seen in other inorganic aromatic clusters studied in our previous works, for example, in  $\text{C}_{4v}$   $\text{NaGa}_4^-$ ,  $D_{4h}$   $\text{Na}_2\text{Ga}_4$ , and  $\text{C}_s$   $\text{Na}_2\text{Ga}_4$ ,<sup>63</sup> as well as in  $\text{C}_{2v}$   $\text{SiAl}_3^-$  and  $\text{GeAl}_3^-$ .<sup>64</sup>

Both the energy difference between the global minimum  $D_{5h}$  structure and the  $\text{C}_{2v}$  isomer and the energies of reactions 1 and 2 decrease from  $\text{P}_5^-$  to  $\text{Sb}_5^-$ , implying that the stability of the  $D_{5h}$  structure relative to the  $\text{C}_{2v}$  structure is reduced for the heavier  $\text{Pn}_5^-$  clusters. This is due to the fact that the aromatic stabilization is weakened for the heavier species as a result of the poorer overlap between the  $\text{np}_z$  atomic orbitals.

The pentagonal structures of the  $\text{Pn}_5^-$  clusters and their aromaticity were established previously.<sup>91–94</sup> In this work we were able to probe deeper MOs in  $\text{Pn}_5^-$  because of the use of high detachment energies and the electron propagator theory. Detailed comparison between the MOs of  $\text{Pn}_5^-$  and  $\text{C}_5\text{H}_5^-$  reveals that while both species are aromatic, their order of the valence MOs is different. In the case of the aromatic hydrocarbon  $\text{C}_5\text{H}_5^-$ , the  $\sigma$ -MOs are filled before the  $\pi$ -MOs, but in the case of  $\text{Pn}_5^-$ , the lowest  $\pi$ -aromatic MO is lower in energy than the  $\sigma$ -MOs, and thus the  $\pi$ -MO is filled before the  $\sigma$ -MOs. This observation may be responsible for the inability of pentapnictogens to form large polycyclic planar aromatic systems, analogous to naphthalene and anthracene. This question will be addressed in the future using large pentapnictogen clusters.

## 8. Conclusions

We have carried out a combined photoelectron spectroscopy and ab initio study of the pentapnictogen  $\text{Pn}_5^-$  ( $\text{Pn} = \text{P}, \text{As}, \text{Sb}, \text{and Bi}$ ) species to elucidate their structure, bonding, and

aromaticity. Well resolved photoelectron spectra were obtained for all the anions at several photon energies. Ab initio calculations showed that all the  $\text{Pn}_5^-$  species have the aromatic cyclic  $D_{5h}$  singlet structure as their ground state with a  $\text{C}_{2v}$  bridged-roof low-lying singlet isomer. We found that the stability of the aromatic planar cyclic structure relative to the  $\text{C}_{2v}$  bridged-roof low-lying isomer decreases from  $\text{P}_5^-$  to  $\text{Sb}_5^-$ , for which both isomers were observed experimentally. Molecular orbital analyses showed that the occupied orbitals in the  $\text{Pn}_5^-$  clusters are similar to those of the isovalent  $\text{C}_5\text{H}_5^-$  with the same set of  $\pi$ -orbitals. However, we found that the  $1a_2''$  orbital (the most stable  $\pi$  orbital) is lower in energy than the upper  $\sigma$ -orbitals in the cyclic  $\text{Pn}_5^-$  species, which is different from the valence isoelectronic hydrocarbon  $\text{C}_5\text{H}_5^-$ , where all the  $\pi$ -orbitals are higher in energy and well separated from the  $\sigma$ -orbitals. This behavior makes inorganic aromatic compounds different from the organic ones.

**Acknowledgment.** The theoretical work was done at Utah State University and partially supported by The Petroleum Research Fund (ACS-PRF# 35255-AC6), administered by the American Chemical Society. The experimental work done at Washington was supported by the National Science Foundation (CHE-9817811) and performed at the W. R. Wiley Environmental Molecular Sciences Laboratory, a national scientific user facility sponsored by DOE's Office of Biological and Environmental Research and located at Pacific Northwest National Laboratory, which is operated for DOE by Battelle.

## References and Notes

- (1) Foust, A. S.; Foster, M. S.; Dahl, L. F. *J. Am. Chem. Soc.* **1969**, *91*, 5633.
- (2) Ginsberg, A. P.; Lindsell, W. E.; McCullough, K. J.; Spinkle, C. R.; Welch, A. J. *J. Am. Chem. Soc.* **1986**, *108*, 403.
- (3) Di Vaira, M.; Sacconi, L. *Angew. Chem., Int. Ed. Engl.* **1982**, *21*, 330.
- (4) Scherer, O. J. *Angew. Chem., Int. Ed. Engl.* **1990**, *29*, 1104.
- (5) Whitmire, K. H. *Adv. Organomet. Chem.* **1998**, *42*, 1.
- (6) Scherer, O. J. *Acc. Chem. Res.* **1999**, *32*, 751.
- (7) Scherer, O. J. *Angew. Chem., Int. Ed.* **2000**, *39*, 1029.
- (8) Scherer, O. J.; Bruck, T. *Angew. Chem., Int. Ed. Engl.* **1987**, *26*, 59.
- (9) Baudler, M.; Duster, D.; Ouzounis, D. *Z. Anorg. Allg. Chem.* **1987**, *544*, 87.
- (10) Baudler, M.; Akpoglugou, S.; Ouzounis, D.; Wasgetian, F.; Meinigke, B.; Budzikiewicz, H.; Munster, H. *Angew. Chem., Int. Ed. Engl.* **1988**, *27*, 280.
- (11) Urnezis E.; Brennessel, W.; Ellis, J. *Abstr. Pap. Am. Chem. Soc.* **2001**, 221, 650-INor. (Abstracts of papers of the American Chemical Society, 221: 650-INOR, Part 1, Apr 1, 2001.)
- (12) Hamilton, T. P.; Schaefer, H. F., III. *Chem. Phys. Lett.* **1990**, *166*, 303.
- (13) Jones, R. O.; Hohl, D. *J. Chem. Phys.* **1990**, *92*, 6710.
- (14) Jones, R. O.; Seifert, G. *J. Chem. Phys.* **1992**, *96*, 7564.
- (15) Seifert, G.; Jones, R. O. *Z. Phys. D* **1993**, *26*, 349.
- (16) Jones, R. O.; Gantefor, G.; Hunsicker, S.; Pieperhoff, P. *J. Chem. Phys.* **1995**, *103*, 9549.
- (17) Warren, D. S.; Gimarc, B. M. *J. Am. Chem. Soc.* **1992**, *114*, 5378.
- (18) Haser, M.; Treutler, O. *J. Chem. Phys.* **1995**, *102*, 3703.
- (19) Hu, C. H.; Shen, M. Z.; Schaefer, H. F., III. *Theor. Chim. Acta* **1994**, *88*, 29.
- (20) Rulisek, L.; Havlas, Z.; Hermanek, S.; Plešek, J. *Can. J. Chem.* **1998**, *76*, 1274.
- (21) Chen, M. D.; Huang, R. B.; Zheng, L. S.; Zhang, Q. E.; Au, C. T. *Chem. Phys. Lett.* **2000**, *325*, 22.
- (22) Chen, M. D.; Huang, R. B.; Zheng, L. S.; Au, C. T. *J. Mol. Struct. (THEOCHEM)* **2000**, *499*, 195.
- (23) Chen, M. D.; Li, J. T.; Huang, R. B.; Zheng, L. S.; Au, C. T. *Chem. Phys. Lett.* **1999**, *305*, 439.
- (24) Glukhovtsev, M. N.; Dransfeld, A.; Schleyer, P. v. R. *J. Phys. Chem.* **1996**, *100*, 13447.
- (25) Glukhovtsev, M. N.; Schleyer, P. v. R.; Maerker, C. *J. Phys. Chem.* **1993**, *97*, 8200.

- (26) Dransfeld, A.; Nyulaszi, L.; Schleyer, P. v. R. *Inorg. Chem.* **1998**, 37, 4413.
- (27) Scuseria, G. E. *J. Chem. Phys.* **1990**, 92, 6722.
- (28) Ballone, P.; Jones, R. O. *J. Chem. Phys.* **1994**, 100, 4941.
- (29) Warren, D. S.; Gimarc, B. M.; Ming, Z. *Inorg. Chem.* **1994**, 33, 710.
- (30) Shen, M. Z.; Schaefer, H. F., III. *J. Chem. Phys.* **1994**, 101, 2261.
- (31) Alcamí, M.; Mo, O.; Yanez, M. J. *J. Chem. Phys.* **1998**, 108, 8957.
- (32) Gausa, M.; Kaschner, R.; Lutz, H. O.; Seifert, G.; Meiwes-Broer, K.-H. *Chem. Phys. Lett.* **1994**, 230, 99.
- (33) Kaschner, R.; Saalmann, U.; Seifert, G.; Gausa, M. *Int. J. Quantum Chem.* **1995**, 56, 771.
- (34) Kumar, V. *Phys. Rev. B* **1993**, 48, 8470.
- (35) Sundararajan, V.; Kumar, V. *J. Chem. Phys.* **1995**, 102, 9631.
- (36) Gonzalez, A. I.; Mo, O.; Yanez, M. J. *J. Chem. Phys.* **2000**, 112, 2258.
- (37) Balasubramanian, K.; Liao, D.-W. *J. Chem. Phys.* **1991**, 95, 3064.
- (38) Balasubramanian, K.; Sumathi, K.; Dai, D. G. *J. Chem. Phys.* **1991**, 95, 3494.
- (39) Zhang, H. X.; Balasubramanian, K. *J. Chem. Phys.* **1992**, 97, 3437.
- (40) Raghavachari, K.; Haddon, R. C.; Binkley, J. S. *Chem. Phys. Lett.* **1985**, 122, 219.
- (41) Ferris, K. F.; Bartlett, R. J. *J. Am. Chem. Soc.* **1992**, 114, 8302.
- (42) Janoschek, R. *Chem. Ber.* **1992**, 125, 2687.
- (43) Kobayashi, K.; Miura, H.; Nagase, S. *J. Mol. Struct. (THEOCHEM)* **1994**, 311, 69.
- (44) Wang, L. S.; Lee, Y. T.; Shirley, D. A.; Balasubramanian, K.; Feng, P. *J. Chem. Phys.* **1990**, 93, 6310.
- (45) Wang, L. S.; Niu, B.; Lee, Y. T.; Shirley, D. A.; Ghelichkhani, E.; Grant, E. R. *J. Chem. Phys.* **1990**, 93, 6318.
- (46) Wang, L. S.; Niu, B.; Lee, Y. T.; Shirley, D. A.; Ghelichkhani, E.; Grant, E. R. *J. Chem. Phys.* **1990**, 93, 6327.
- (47) Yoo, R. K.; Ruscic, B.; Berkowitz, J. J. *Electron. Spectrosc.* **1993**, 66, 39.
- (48) Bulgakov, A. V.; Bobrenok, O. F.; Kosyakov, V. I. *Chem. Phys. Lett.* **2000**, 320, 19.
- (49) Schroder, D.; Sachwarz, H.; Wulf, M.; Sievers, H.; Jutzi, P.; Reiher, M. *Angew. Chem., Int. Ed. Engl.* **1999**, 38, 3513.
- (50) Bennett, S. L.; Margrave, J. L.; Franklin, J. L.; Hudson, J. E. *J. Chem. Phys.* **1973**, 59, 5814.
- (51) Yoo, R. K.; Ruscic, B.; Berkowitz, J. J. *J. Chem. Phys.* **1992**, 96, 6696.
- (52) Lippa, T. P.; Xu, S.-J.; Lyapustina, S. A.; Nilles, J. M.; Bowen, K. H. *J. Chem. Phys.* **1998**, 109, 10727.
- (53) Sattler, K.; Munlbach, J.; Recknagel, E. *Phys. Rev. Lett.* **1980**, 45, 821.
- (54) Geusic, M. E.; Freeman, R. R.; Duncan, M. A. *J. Chem. Phys.* **1988**, 88, 163.
- (55) Geusic, M. E.; Freeman, R. R.; Duncan, M. A. *J. Chem. Phys.* **1988**, 89, 223.
- (56) Rayane, D.; Melinon, P.; Tribollet, B.; Cabaud, B.; Hoareau, A.; Broyer, M. *J. Chem. Phys.* **1989**, 91, 3100.
- (57) Polak, M. L.; Gerber, G.; Ho, J.; Lineberger, W. C. *J. Chem. Phys.* **1992**, 97, 8990.
- (58) Gausa, M.; Kaschner, R.; Seifert, G.; Faehrmann, J. H.; Lutz, H. O.; Meiwes-Broer, K.-H. *J. Chem. Phys.* **1996**, 104, 9719.
- (59) Walstedt, R. E.; Bell, R. F. *Phys. Rev. A* **1986**, 33, 2830.
- (60) Polak, M. L.; Ho, J.; Gerber, G.; Lineberger, W. C. *J. Chem. Phys.* **1991**, 95, 3053.
- (61) For a review see: Boldyrev, A. I.; Wang, L. S. *J. Phys. Chem. A* **2001**, 105, 10759.
- (62) Li, X.; Kuznetsov, A. E.; Zhang, H. F.; Boldyrev, A. I.; Wang, L. S. *Science* **2001**, 291, 859.
- (63) Kuznetsov, A. E.; Boldyrev, A. I.; Li, X.; Wang, L. S. *J. Am. Chem. Soc.* **2001**, 123, 8825.
- (64) Li, X.; Zhang, H. F.; Wang, L. S.; Kuznetsov, A. E.; Cannon, N. A.; Boldyrev, A. I. *Angew. Chem., Int. Ed.* **2001**, 40, 1867.
- (65) Kuznetsov, A. E.; Corbett, J. D.; Wang, L. S.; Boldyrev, A. I. *Angew. Chem., Int. Ed.* **2001**, 40, 3369.
- (66) Wang, L. S.; Cheng, H. S.; Fan, J. J. *J. Chem. Phys.* **1995**, 102, 9480.
- (67) Wang, L. S.; Wu, H. In *Advances in Metal and Semiconductor Clusters. IV. Cluster Materials*; Duncan, M. A., Ed.; JAI Press: Greenwich, 1998; p 299.
- (68) Hotop, H.; Lineberger, W. C. *J. Phys. Chem. Ref. Data* **1985**, 14, 731.
- (69) McLean, A. D.; Chandler, G. S. *J. Chem. Phys.* **1980**, 72, 5639.
- (70) Clark, T.; Chandrasekhar, J.; Spitznagel, G. W.; Schleyer, P. v. R. *J. Comput. Chem.* **1983**, 4, 294.
- (71) Frisch, M. J.; Pople, J. A.; Binkley, J. S. *J. Chem. Phys.* **1984**, 80, 3265.
- (72) Binkley, J. S.; Pople, J. A.; Hehre, W. J. *J. Am. Chem. Soc.* **1980**, 102, 939.
- (73) Gordon, M. S.; Binkley, J. S.; Pople, J. A.; Pietro, W. J.; Hehre, W. J. *J. Am. Chem. Soc.* **1982**, 104, 2797.
- (74) Pietro, W. J.; Franchi, M. M.; Hehre, W. J.; Defrees, D. J.; Pople, J. A.; Binkley, J. S. *J. Am. Chem. Soc.* **1982**, 104, 5039.
- (75) Dobbs, K. D.; Hehre, W. J. *J. Comput. Chem.* **1986**, 7, 359.
- (76) Dobbs, K. D.; Hehre, W. J. *J. Comput. Chem.* **1987**, 8, 861.
- (77) Dobbs, K. D.; Hehre, W. J. *J. Comput. Chem.* **1987**, 8, 880.
- (78) Parr, R. G.; Yang, W. *Density-functional theory of atoms and molecules*; Oxford University Press: Oxford, 1989.
- (79) Becke, A. D. *J. Chem. Phys.* **1993**, 98, 5648.
- (80) Perdew, J. P.; Chevary, J. A.; Vosko, S. H.; Jackson, K. A.; Pederson, M. R.; Singh, D. J.; Fiolhais, C. *Phys. Rev. B* **1992**, 46, 6671.
- (81) Cizek, J. *Adv. Chem. Phys.* **1969**, 14, 35.
- (82) Purvis, G. D., III; Bartlett, R. J. *J. Chem. Phys.* **1982**, 76, 1910.
- (83) Scuseria, G. E.; Janssen, C. L.; Schaefer, H. F., III. *J. Chem. Phys.* **1988**, 89, 7282.
- (84) Cederbaum, L. S. *J. Phys. B* **1975**, 8, 290.
- (85) Niessen, W. von; Shirmir, J.; Cederbaum, L. S. *Comput. Phys. Rep.* **1984**, 1, 57.
- (86) Zakrzewski, V. G.; Niessen, W. von. *J. Comput. Chem.* **1993**, 14, 13.
- (87) Zakrzewski, V. G.; Ortiz, J. V. *Int. J. Quantum Chem.* **1995**, 53, 583.
- (88) For a recent review see: Ortiz, J. V.; Zakrzewski, V. G.; Dolgunitcheva, O. In *Conceptual Trends in Quantum Chemistry*; Kryachko, E. S., Ed.; Kluwer: Dordrecht, 1997; Vol. 3, p 463.
- (89) Frisch, M. J.; Trucks, G. M.; Schlegel, H. B.; Scuseria, G. E.; Robb, M. A.; Cheeseman, J. R.; Zakrzewski, V. G.; Montgomery, J. A., Jr.; Stratmann, R. E.; Burant, J. C.; Dapprich, S.; Millam, J. M.; Daniels, A. D.; Kudin, K. N.; Strain, M. C.; Farkas, O.; Tomasi, J.; Barone, V.; Cossi, M.; Cammi, R.; Mennucci, B.; Pomelli, C.; Adamo, C.; Clifford, S.; Ochterski, J.; Petersson, G. A.; Ayala, P. Y.; Cui, Q.; Morokuma, K.; Malick, D. K.; Rabuck, A. D.; Raghavachari, K.; Foresman, J. B.; Cioslowski, J.; Ortiz, J. V.; Baboul, A. G.; Stefanov, B. B.; Liu, G.; Liashenko, A.; Piskorz, P.; Komaromi, I.; Gomperts, R.; Martin, R. L.; Fox, D. J.; Keith, T.; Al-Laham, M. A.; Peng, C. Y.; Nanayakkara, A.; Gonzalez, C.; Challacombe, M.; Gill, P. M. W.; Johnson, B. G.; Chen, W.; Wong, M. W.; Andres, J. L.; Head-Gordon, M.; Replogle, E. S.; Pople, J. A. *Gaussian 98* (revision A.7); Gaussian, Inc.: Pittsburgh, PA, 1998.
- (90) Schaftenaar, G. *MOLDEN3.4*, CAOS/CAMM Center, The Netherlands, 1998.
- (91) Scherer, O. J. *Angew. Chem., Int. Ed. Engl.* **1990**, 29, 1104.
- (92) Urnezis, E.; Brennessel, W. W.; Cremer, C. J.; Ellis, J. E.; Schleyer, P. v. R. *Science* **2002**, 295, 832.
- (93) Malar, E. J. P. *J. Org. Chem.* **1992**, 57, 3694.
- (94) Dransfeld, A.; Nyulazi, L.; Schleyer, P. v. R. *Inorg. Chem.* **1998**, 37, 4413.